Journal of
Intelligent Material
Systems and Structures

Original Article

Journal of Intelligent Material Systems and Structures
2014, Vol. 25(12) 1456–1468

DOI: 10.1177/1045389X13507343
jim.sagepub.com
SAGE

Nonlinear multiclass support vector machine–based health monitoring system for buildings employing magnetorheological dampers

Jo Woon Chong[1], Yeesock Kim[2] and Ki H Chon[3]

Abstract

In this article, a nonlinear multiclass support vector machine–based structural health monitoring system for smart structures is proposed. It is developed through the integration of a nonlinear multiclass support vector machine, discrete wavelet transforms, autoregressive models, and damage-sensitive features. The discrete wavelet transform is first applied to signals obtained from both healthy and damaged smart structures under random excitations, and it generates wavelet-filtered signal. It not only compresses lengthy data but also filters noise from the original data. Based on the wavelet-filtered signals, several wavelet-based autoregressive models are then constructed. Next, damage-sensitive features are extracted from the wavelet-based autoregressive coefficients and then the nonlinear multiclass support vector machine is trained by a variety of damage levels of wavelet-based autoregressive coefficient sets in an optimal method. The trained nonlinear multiclass support vector machine takes new test wavelet-based autoregressive coefficients that are not used in the training process and quantitatively estimates the damage levels. To demonstrate the effectiveness of the proposed nonlinear multiclass support vector machine, a three-story smart building equipped with a magnetorheological damper is studied. As a baseline, naive Bayes classifier–based structural health monitoring system is presented. It is shown from the simulation that the proposed nonlinear multiclass support vector machine–based approach is efficient and precise in quantitatively estimating damage statuses of the smart structures.

Keywords

Autoregressive, discrete wavelet transform, earthquake engineering, magnetorheological damper, nonlinear multiclass support vector machine, smart structure, structural health monitoring

Introduction

Nonlinear multiclass support vector machine

In recent years, support vector machine (SVM) has received much attention from a variety of engineering fields. In particular, SVM has recently attracted the attention of civil engineering scholars. The reason is that it is effective in dealing with the classification of incomplete and noisy measurements obtained from large-scale civil structures; Oh and Sohn (2009) integrated an SVM with a principal component analysis, an autoregressive (AR)-AR exogenous (ARX) model, and a sequential probability ratio test process. The integrated process compares the AR-ARX coefficients obtained from the undamaged and damaged dynamic systems. The damage detection performance is evaluated in the presence of an unmeasured operational variation. Park et al. (2006) applied a radial basis function to nonlinear SVM-based binary classification for damage detection of small-scale steel bridge components. The key to the method is comparing the maximum peak values of the reconstructed wavelet signals at a specific frequency. They demonstrated that the SVM is effective in classifying the ambiguous class regions. He and Yan (2007) proposed the wavelet-based SVM for damage detection of a single-layer spherical lattice dome under ambient excitations. The

[1]Laboratory for Information and Decision Systems, Massachusetts Institute of Technology (MIT), Cambridge, MA, USA
[2]Department of Civil & Environmental Engineering, Worcester Polytechnic Institute (WPI), Worcester, MA, USA
[3]Department of Biomedical Engineering, Worcester Polytechnic Institute (WPI), Worcester, MA, USA

Corresponding author:
Yeesock Kim, Department of Civil & Environmental Engineering, Worcester Polytechnic Institute (WPI), Worcester, MA 01609, USA.
Email: yeesock@wpi.edu

SVMs are trained using damage-sensitive feature (DSF) vectors obtained from the dynamic responses. It has also been demonstrated from experimental studies that an SVM can be effective in estimating steel bridge rust (Chen et al., 2012). They extracted two features of the background surface and the damaged surface (i.e. rust pixels) using the Fourier transform and the Gaussian low-pass filter. Then, a binary-type SVM effectively identified the different features of the rust (i.e. damage) and background. The binary SVM has also been used for detection of abnormality on a cable-stayed bridge structure located in an inner gulf of Zhanjiang City in south China (Vines-Cavanaugh et al., 2010). The SVM was used to identify whether the east end expansion joint of the bridge was normal. It also classified whether the longitudinal motion of the main girder was constrained or not. Chen et al. (2012a, 2012b) proposed a new evolutionary SVM by integrating SVM and a fast messy genetic algorithm (fmGA). They used the fmGAs for the performance evaluation of school buildings in seismic zones of Taiwan. The fmGA-SVM was trained using performance-target ground accelerations expressed in terms of design response spectrums, performance points, equivalent basic period, and equivalent damping ratio. Bulut et al. (2005) studied the effectiveness of SVM applications for damage detection of the Humboldt Bay Middle Channel Bridge. To generate the data sets for training SVMs, a finite element model (FEM) employing perfect hinge elements under hammer-like forces was constructed. The signals obtained from the FEM were preprocessed first using the wavelet transform and then the SVM classifier was used to detect the location of damage with a high degree of accuracy. In other examples, many attempts have been made by Mita and colleagues to apply SVM to detecting damage in a variety of systems, including a five-story shear-type building structure (Mita and Hagiwara, 2003; Shimada and Mita, 2005), a power distribution pole with various boundary conditions (Shimada et al., 2006), a fiber Bragg grating (FBG) sensor imbedded structure (Hayano and Mita, 2005), and two aluminum plates joined by bolts employing piezoelectric (lead zirconate titanate (PZT)) sensors (Mita and Taniguchi, 2004).

However, all the aforementioned SVM models have been applied based on the assumption that the structure under investigation is linear and time-invariant (LTI). There is no nonlinear multiclassification using SVM on time-varying nonlinear dynamic systems (e.g. smart structures equipped with highly nonlinear hysteretic control devices) under ambient excitations.

Monitoring of smart structures

Control technology has recently been used in large-scale civil structures because behavior of structural systems can be modified to counter destructive environmental loadings without significantly increasing the mass of the structure (Adeli and Saleh, 1999; Mitchell et al. 2012). In this context, smart structures using semiactive control devices have received great attention because they combine the best features of passive and active control systems (Dyke et al., 1996; Kim et al., 2009a, 2009b, 2011; Nagarajaiah and Spencer, 2003; Spencer et al., 1997). However, the performance of the smart structures can degrade in the presence of structure/sensor/actuator faults Ankireddi and Yang 1999; Li et al., 2007; (Sharifi et al., 2010).

Yun and Masri (2008, 2009) have provided an application example on how nonlinear smart control devices can be monitored. For example, they proposed an effective method for damage detection of magnetorheological (MR) dampers using the restoring force method (RFM). It was shown that the RFM coefficients (in particular, orthogonal coefficients) can be used as DSFs of the MR dampers. Unfortunately, no systematic approach for structural health monitoring (SHM) has been investigated to identify structural damage of buildings equipped with MR dampers under ambient excitations. In particular, there is no comprehensive report on using nonlinear multiclass SVMs (NMSVMs) for damage detection of buildings employing MR dampers (Kim et al., 2013b). Therefore, the discussion in this article will center on developing a novel NMSVM-based SHM framework for damage detection of buildings employing MR dampers under ambient excitations.

This article is organized as follows: section "Multiclass classification" describes the NMSVM algorithm in detail. Section "Statistical pattern" discusses the pattern extraction process, including wavelet transform, the AR model, and DSFs. Simulation results are given in section "Case study: smart structures." Finally, concluding remarks are given in section "Conclusion."

Multiclass classification

In this section, NMSVM-based classification algorithms are described for SHM of smart buildings with a highly nonlinear time-varying damping device. Since the SVM-based classification results are compared with naive Bayes (NB) approach, NB classifiers are first described in section "NB classifiers"; then multiclass SVM-based classification is described in section "SVM classifier."

NB classifiers

The NB classifier first trains itself by formulating a probability distribution function of $P\{\zeta|S_k\}$, $k = 1, \ldots, N_S$, with the given training data points $\zeta_{tr}, tr = 1, \ldots, N_T$ and their corresponding target variable $\tau_{tr} \in \{S_1, \ldots, S_{N_S}\}$, where N_{tr} is the number of training data points and N_S is the number of classes. A Gaussian function is widely adopted for $P\{\zeta|S_k\}$

$$P\{\zeta|S_k\} = \frac{1}{\sqrt{2\pi}\sigma_k} e^{\frac{-(\zeta-\mu_k)^2}{2\sigma_k{}^2}} \quad (1)$$

where μ_k and σ_k denote the mean and variance of class S_k, respectively. Hence, training the Gaussian function–based NB classifier becomes deriving the sample mean and variance in ζ_{tr} for each class S_k. Then, the trained NB classifier classifies unknown test input data based on the following Bayesian theorem

$$P\{U|\zeta_{te}\} \propto P\{\zeta_{te}|U\}P\{U\} \quad (2)$$

where ζ_{te} are the unknown test data points and $U \in \{S_1, \ldots, S_{N_S}\}$ are their corresponding estimated target variable. Specifically, the trained NB classifier determines the class τ_{te} of new input data ζ_{te} as

$$\tau_{te} = \underset{U\in\{S_1,\ldots,S_{N_S}\}}{\arg\max} \; P\{U|\zeta_{te}\} \quad (3)$$

This NB classifier is used as a baseline. Its performance is compared with the NMSVM approach in terms of training and validation errors in classifying a variety of damage levels in nonlinear time-varying smart buildings.

SVM classifier

Binary SVM. The SVM classifier that finds support vectors for two classes (damage and health) is first trained so that the distance between two classes is maximized. A SVM can be categorized as either a hard-margin SVM or a soft-margin SVM, where the margin is defined as the smallest distance between the training data and the decision boundary. A hard-margin SVM can only be applied to completely separable training data sets. The support vectors of the hard-margin SVM can be found by the following equation

$$\begin{aligned}&\text{Minimize } d_{\text{SVM}}(\mathbf{w}_s) = \frac{1}{2}\langle \mathbf{w}_s, \mathbf{w}_s\rangle \\ &\text{Subject to } \tau_{tr}(\langle \mathbf{w}_s, \zeta_{tr}\rangle + b_s) \geq 1, \quad \text{for } tr = 1, 2, \ldots, N_T\end{aligned} \quad (4)$$

where $\mathbf{w}_s \in \mathbf{R}^O$ is the weight vector, $\zeta_{tr} \in \mathbf{R}^O$ is the trth input vector data, $\tau_{tr} \in \{1, -1\}$ is the trth target variable, $b_s \in \mathbf{R}$ is the bias, and $\langle \mathbf{w}_s, \zeta_{tr}\rangle$ is the inner product operation of $\mathbf{w}_s$ and ζ_{tr}. With these support vectors, the decision boundary F_{sv} is derived as

$$F_{sv} = \langle \mathbf{w}_s^*, \zeta\rangle + b_s^* = 0 \quad (5)$$

where $\mathbf{w}_s^*$ and b_s^* are the weight vector and bias, respectively, obtained from equation (4), and ζ is the input point.

A soft-margin SVM can be applied to completely nonseparable training data sets. A soft-margin SVM introduces slack variables $\delta_{tr} = |\tau_{tr} - F_{tr}(\zeta_{tr})|$, $tr = 1, \ldots, N_T$ to control the trade-off between minimizing the misclassification errors and maximizing the margin by parameter C_{SVM}. The support vectors of the soft-margin SVM can be derived by solving the following equations

$$\begin{aligned}&\text{Minimize } d_{\text{SVM}}(\mathbf{w}_s) = \frac{1}{2}\langle \mathbf{w}_s, \mathbf{w}_s\rangle + C_{\text{SVM}} \sum \delta_{tr} \\ &\text{Subject to } \tau_{tr}(\langle \mathbf{w}_s, \zeta_{tr}\rangle + b_s) \geq 1 - \delta_{tr}, \\ &\text{for } tr = 1, 2, \ldots, N_T, \text{ for } \delta_{tr} \geq 0\end{aligned} \quad (6)$$

The corresponding decision boundary of a soft-margin SVM can be obtained using equation (5). The linear SVM can be extended to a nonlinear SVM by introducing the nonlinear mapping $\zeta_{tr} \to \Phi(\zeta_{tr})$ (Burges, 1998). In the nonlinear SVM, the constraint in equation (4) is substituted into

$$\tau_{tr}(\langle \mathbf{w}_s, \Phi(\zeta_{tr})\rangle + b_s) \geq 1, \quad \text{for } tr = 1, 2, \ldots, N \quad (7)$$

To facilitate the operation for a nonlinear SVM, a kernel function K_s, which is a dot-product in the transformed feature space, is used

$$K_s(\zeta_{tr}, \zeta_{tr'}) = \langle \Phi(\zeta_{tr}), \Phi(\zeta_{tr'})\rangle \quad (8)$$

where $tr' = 1, 2, \ldots, N_T$. The Gaussian radial basis function is used in a variety of fields and its associated kernel is expressed as

$$K_s(\zeta_{tr}, \zeta_{tr'}) = \exp\left(-\frac{\|\zeta_{tr} - \zeta_{tr'}\|^2}{2\sigma^2}\right) \quad (9)$$

where σ is the kernel variance. This nonlinear SVM is applied to the multiclassification problem for damage detection of nonlinear time-varying dynamic systems.

Multiclass SVM. There is a *one-versus-one* classifier as a method for multiclass classification. It trains all the possible pairs of classes. In other words, there exist $M(M-1)/2$ classifiers. Each discriminant function is derived by training the data points from the S_k class as positive and the data points from the S_j class as negative. With this training on each class, the *one-versus-one* classifies the class of input point ζ to the class that has the maximum *votes* (Maimon and Rokach, 2010).

Another possible approach for multiclass classification is the *one-versus-the-rest* classifier. It trains the kth discriminant function by labeling the data points from S_k as positive, while the data points from the other $M-1$ classes ($\{S_1, \ldots, S_{k-1}, S_{k+1}, \ldots, S_{N_S}\}$) as negative. With this training in each class S_k, the *one-versus-the-rest* classifier predicts the class τ of input point ζ as

$$\tau = \underset{U\in\{S_1,\ldots,S_{N_S}\}}{\arg\max} \; \langle \mathbf{w}_{U,s}^*, \zeta\rangle + b_{U,s}^* \quad (10)$$

where $\mathbf{w}_{U,s}^*$ and $b_{U,s}^*$ are the weight vector and bias for class U, respectively, obtained from equation (4). In this article, the *one-versus-the-rest* classifier is adopted due to the low complexity compared to the *one-versus-one* classifier.

Statistical pattern

To generate the data for training the proposed multi-class SVM, a systematic data normalization framework is presented in this section. Figure 1 shows the conceptual configuration of the proposed SHM process. Note that the proposed method is to extract dynamic characteristics of a structure–MR damper system, and thus, the input signals that are applied to the integrated structure–MR damper system need to be random. To this end, the MR damper is operated by a random current signal generator and not a controller with specific band-limited frequencies. The applied disturbance signal is created by a random earthquake generator. First, the discrete wavelet transform (DWT) is applied to dynamic responses of the targeted structure under the random earthquake disturbance and random current signals. The DWT reduces the computational loads and filters noise from the measured data. Then, the wavelet-filtered responses are estimated using AR time series models. Once the wavelet-based AR (WAR) is constructed, the AR coefficients from the WAR model are extracted to identify structural damages. Finally, the extracted features are input to the proposed multi-class SVM algorithm. It is also noted that the MR damper is a nonlinear time-varying dynamic system. Once the MR damper is installed on the structure, the integrated structure–MR damper system behaves nonlinearly even though the structure itself remains linear. Hence, the time-varying stiffness and damping capacities produced by the MR damper that provides a feedback to structures will influence the behavior of structures, resulting in changes in the WAR model. Therefore, many experimental tests need to be conducted. Another important issue to be addressed is that it is critical to maintain the MR damper temperature because the dissipative energy by the MR damper operation increases significantly with increasing temperature of MR fluids during testing. More detailed description can be found in Yun and Masri (2008).

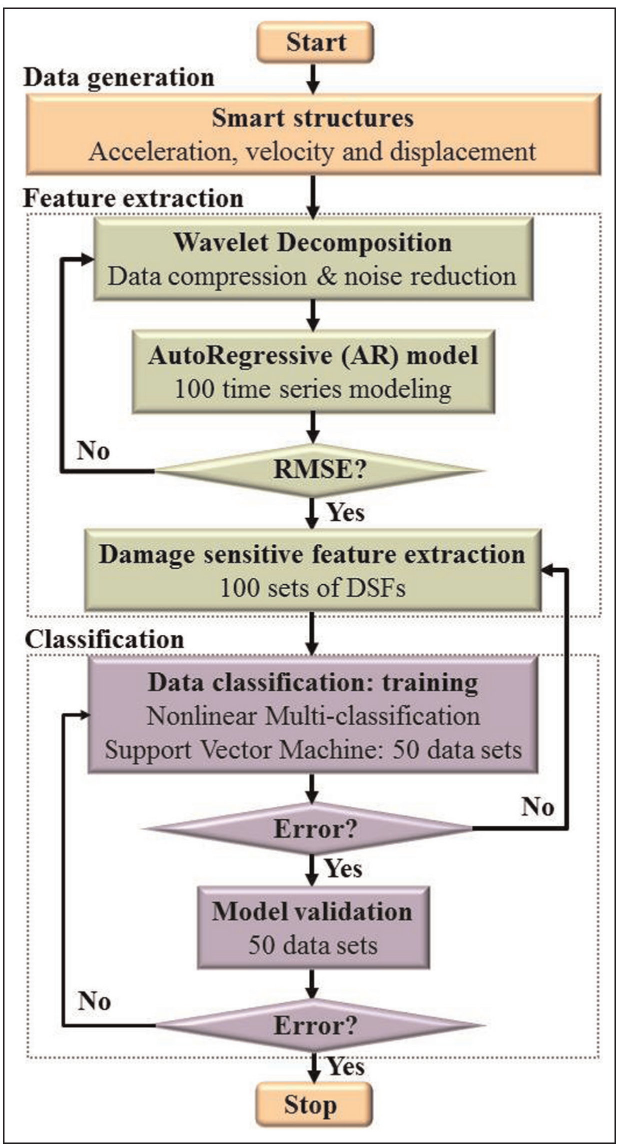

Figure 1. Architecture of the proposed SHM scheme for smart structures.
SHM: structural health monitoring; RMSE: root mean square error; DSF: damage-sensitive feature.

DWT

As a time–frequency analysis method, the DWT can be defined as

$$W_{s_1,s_2} = 2^{-s_1/2} \sum_{s_1} \sum_{s_2} f(n)\psi(2^{-s_1}n - s_2) \qquad (11)$$

where $f(n)$, s_1, and s_2 are an arbitrary time series signal, the scaling factor, and the translation factor, respectively. The DWT decomposes the time series signals obtained from the smart structure into both low- and high-frequency components at different resolutions. The newly decomposed signals consist of approximation (low frequency) and detailed components (high frequency). The approximation and detailed signals are represented with scale and wavelet functions. The scaling function $\phi(n)$ and the wavelet function $\psi(n)$ can be defined as dilation equations

$$\phi_{s_1,s_2} = 2^{-s_1/2}\phi(2^{-s_1}n - s_2) \qquad (12)$$

$$\psi_{s_1,s_2} = 2^{-s_1/2}\psi(2^{-s_1}n - s_2) \qquad (13)$$

As a low-pass filter, the scaling function provides an approximate time series in the AR modeling process, while the corresponding wavelet acts as a high-pass filter, providing the detailed information. In this study, a second-level wavelet filter using the Daubechie scaling function is applied to time series data for noise reduction and data compression. Several levels and types of wavelets were considered. Of those various scaling functions considered, the second-level wavelet decomposition using the Daubechie scaling function appeared to be most effective. The filtered data are used in our AR model.

AR model

A general expression describing the AR model may be written as

$$\mathbf{y}_t = \sum_{k_r=0}^{P} a_{k_r} y_{t-k_r} + e_t \tag{14}$$

where y_{t-k_r}, P, and e_t are output signals, the maximum AR model order, and a noise source or prediction error term, respectively. The coefficient a_{k_r} is estimated using the least squares algorithm

$$\mathbf{y}_t = \boldsymbol{\theta}_l^T \mathbf{H} + \mathbf{e}_t \tag{15}$$

where $\boldsymbol{\theta}_l$ is the coefficient matrix estimate of the AR model. The solution can be found by a minimum error formulation in the least squares sense

$$\text{Min } J_N(\boldsymbol{\theta}_l) = [\mathbf{y}_t - \boldsymbol{\theta}_l^T \mathbf{H}]^2 \tag{16}$$

where $\mathbf{H} = [h_0, h_1, \ldots, h_R]$ and $\boldsymbol{\theta}_l = [g_0, g_1, \ldots, g_R]^T$. $\mathbf{H}$ is composed of R vectors of different delays, and R is the number of selected linearly independent vectors and g_i is the optimal estimate of the AR model coefficients. A more detailed description is provided in Lu et al. (2001). The quadratic objective function in equation (16) is minimized analytically with respect to $\boldsymbol{\theta}_l$

$$\hat{\boldsymbol{\theta}}_l = [\mathbf{H}\mathbf{H}^T]^{-1}\mathbf{H}\mathbf{y}_t \tag{17}$$

As previously discussed, to improve the efficiency of AR modeling using big data sets, the DWT is integrated with the AR modeling framework. The integration of the DWT with the AR modeling process increases the modeling efficiency as well as reduces the amount of data noise.

WAR model

When the DWT is integrated with the AR model, the efficiency of the time series modeling process is enhanced because the DWT is useful to decompose large data sets into subcomponents in terms of both time and frequency (Mitchell et al., 2013). The WAR can be derived as

$$\hat{\mathbf{y}}_t = \sum_{k_r=0}^{P} a_{k_r} W_{s_1, s_2, t-k_r} + \mathbf{e}_t \tag{18}$$

In this study, the WAR model uses level 2 wavelet-filtered signals. As previously discussed, several level wavelets were considered. Of those various scaling functions considered, the second-level wavelet-filtered signals appeared to be most effective. The WAR coefficients are transformed into a set of frequencies or poles.

In general, any damage to a structure will lead to changes in the stiffness and damping of the smart structural system. The changes can be detected by observing the migration patterns of the system frequencies. A statistical decision-making model that can classify the damage can be developed when the AR parameters of both the damaged and undamaged dynamic systems are available because the AR coefficients correspond to frequencies of structures (Nair et al., 2006; Nair and Kiremidjian, 2007). However, the use of the first few AR coefficients would not be effective in detecting any damage to the nonlinear time-varying dynamic systems such as structures equipped with nonlinear hysteretic control devices. With this in mind, a new DSF is extracted from the AR parameters estimated from the velocity responses of the smart structure.

DSF extraction

In this article, a DSF is extracted by normalizing the WAR coefficients. Through various simulations on sensitivity of damage features, normalization of the WAR coefficients using a pseudo-energy expression with velocity responses appeared to be the most effective. The proposed DSF is given by

$$\text{DSF} = \frac{\sum_q^P \frac{1}{2} m \left| V_q^E \right|^2}{\max\left\{ \sum_q^P \frac{1}{2} m \left| V_q^E \right|^2 \right\}} \tag{19}$$

where m is the structural mass and V_q^E is the qth WAR coefficient obtained from the velocity responses. In this study, 1100 DSFs are obtained using the 1100 WAR models from the healthy and smart structures with damage of 5%, 10%, 15%, 30%, and 50% at either the first or second floor. The proposed NMSVM is used to classify the measured data into undamaged and damaged (based on 5%, 10%, 15%, 30%, and 50% stiffness degradation).

Case study: smart structures

MR damper

In recent years, smart control systems have been proposed for large civil structures because they combine the best features of both active and passive control systems (Kim et al., 2010a, 2010b, 2010c; Nagarajaiah and Spencer, 2003). In particular, one of the controllable

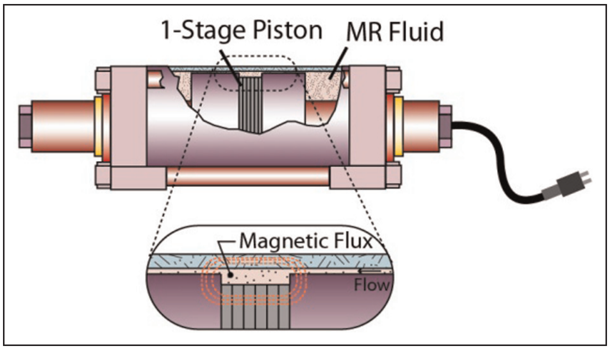

Figure 2. MR damper.
MR: magnetorheological.

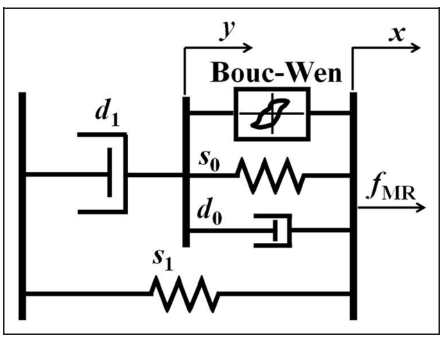

Figure 3. Schematic representation of the mathematical model for the MR damper.
MR: magnetorheological.

fluid dampers, an MR damper as shown in Figure 2, has attracted considerable attention in recent years due to its appealing characteristics: reliable operation, fast response time, low power requirements, broad temperature range, adjustable operating points, and low manufacturing cost (Hurlebaus and Gaul, 2006; Spencer et al., 1997).

To fully use the best features of the MR damper, Spencer et al. (1997) proposed a Bouc–Wen type model, as shown in Figure 3.

The MR damper force $f_{MR}(t)$ is given by

$$f_{MR} = d_1\dot{y} + s_1(x - x_0) \tag{20}$$

$$\dot{z}_{BW} = -\gamma|\dot{x} - \dot{y}|z_{BW}|z_{BW}|^{n-1} - \beta(\dot{x} - \dot{y})|z_{BW}|^n + A(\dot{x} - \dot{y}) \tag{21}$$

$$\dot{y} = \frac{1}{(d_0 + d_1)}\{\alpha z_{BW} + d_0\dot{x} + s_0(x - y)\} \tag{22}$$

$$\alpha = \alpha_a + \alpha_b u \tag{23}$$

$$d_1 = d_{1a} + d_{1b}u \tag{24}$$

$$d_0 = d_{0a} + d_{0b}u \tag{25}$$

$$\dot{u} = -\eta(u - v) \tag{26}$$

where z_{BW} and α, called evolutionary variables, describe the hysteretic behavior of the MR damper; d_0 is the viscous damping parameter at high velocities; d_1 is the viscous damping parameter for the force roll-off at low velocities; α_a, α_b, d_{0a}, d_{0b}, d_{1a}, and d_{1b} are parameters that account for the dependence of the MR damper force on the voltage applied to the current driver; s_0 controls the stiffness at large velocities; s_1 represents the accumulator stiffness; x_0 is the initial displacement of the spring stiffness s_1; γ, β, n, and A are adjustable shape parameters of the hysteresis loops, that is, the linearity in the unloading and the transition between pre-yielding and post-yielding regions; v and u are input and output voltages of a first-order filter, respectively; and η is the time constant of the first-order filter. Note that nonlinear phenomena occur when highly nonlinear MR dampers are applied to structural systems for effective energy dissipation. Such an integrated structure–MR damper system behaves nonlinearly although the structure itself is usually assumed to behave linearly (Arsava et al., 2013a). Therefore, it is challenging to detect structural damage using the migration of frequencies due to the characteristics of the nonlinear time-varying dynamic system. In other words, frequencies of the nonlinear time-varying dynamic system can change even though there is no damage in the structural system.

A building equipped with an MR damper

Figure 4 shows a typical building equipped with an MR damper.

The equation of motion of the integrated smart structure is given by

$$\mathbf{M}\ddot{\mathbf{y}}_s + \mathbf{C}\dot{\mathbf{y}}_s + \mathbf{K}\mathbf{y}_s = \Gamma\mathbf{f}_{\mathbf{MR}}(t, y_{si}, \dot{y}_{si}, v_1) - \mathbf{M}\Lambda\ddot{w}_g \tag{27}$$

where $\ddot{w}_g$ is the earthquake disturbance; **M**, **K**, and **C** are the mass, stiffness, and damping matrices, respectively; $\mathbf{y}_s$, $\dot{\mathbf{y}}_s$, and $\ddot{\mathbf{y}}_s$ are the displacement, velocity, and acceleration relative to the ground, respectively; y_{si} and $\dot{y}_{si}$ are the displacement and the velocity at the ith floor level relative to the ground, respectively; v_1 is the voltage level to be applied; and Γ and Λ are the control and disturbance location vectors, respectively. Figure 5 shows the conceptual configuration of the integrated building–MR damper system.

The second-order differential equation is converted into a first-order differential one

$$\begin{aligned} \dot{\mathbf{z}}_s &= \mathbf{A}^*\mathbf{z}_s + \mathbf{B}^*\mathbf{f}_{\mathbf{MR}}(t, z_{s1}, z_{s4}, v_1) - \mathbf{E}^*\ddot{w}_g \\ \mathbf{y} &= \mathbf{C}^*\mathbf{z}_s + \mathbf{D}^*\mathbf{f}_{\mathbf{MR}}(t, z_{s1}, z_{s4}, v_1) + \mathbf{n} \end{aligned} \tag{28}$$

where

$$\mathbf{A}^* = \begin{bmatrix} \mathbf{0} & \mathbf{I} \\ -\mathbf{M}^{-1}\mathbf{K} & -\mathbf{M}^{-1}\mathbf{C} \end{bmatrix} \tag{29}$$

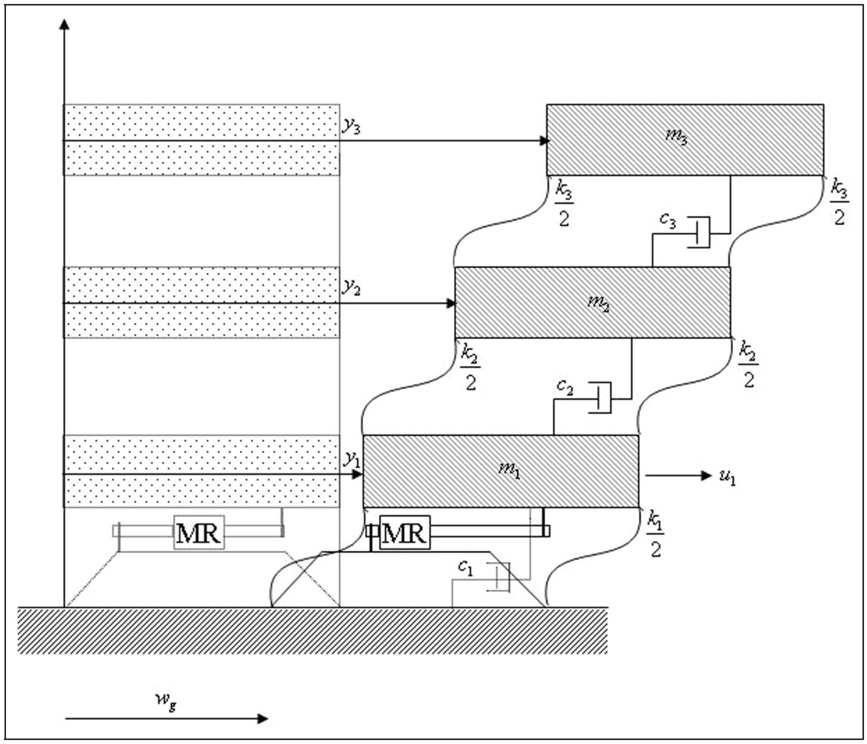

Figure 4. Smart building equipped with MR dampers.
MR: magnetorheological.

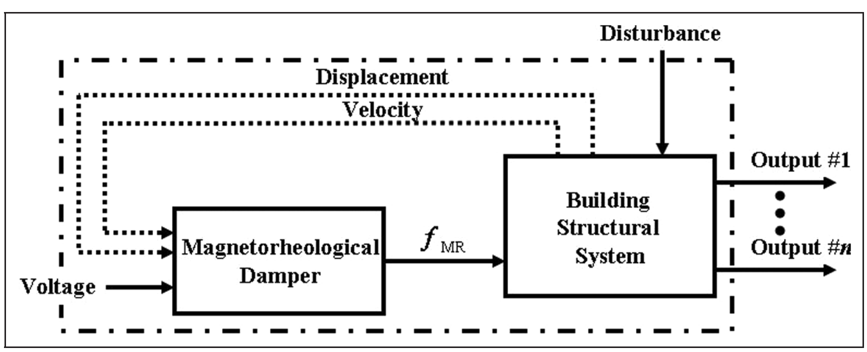

Figure 5. Integrated building structure–MR damper system.
MR: magnetorheological.

$$\mathbf{B}^* = \begin{bmatrix} \mathbf{0} \\ \mathbf{M}^{-1}\mathbf{F} \end{bmatrix} \tag{30}$$

$$\mathbf{C}^* = \begin{bmatrix} \mathbf{I} & \mathbf{0} \\ \mathbf{0} & \mathbf{I} \\ -\mathbf{M}^{-1}\mathbf{K} & -\mathbf{M}^{-1}\mathbf{C} \end{bmatrix} \tag{31}$$

$$\mathbf{D}^* = \begin{bmatrix} \mathbf{0} \\ \mathbf{0} \\ \mathbf{M}^{-1}\mathbf{F} \end{bmatrix} \tag{32}$$

$$\mathbf{E}^* = \begin{bmatrix} \mathbf{0} \\ \mathbf{F} \end{bmatrix} \tag{33}$$

where **F** is the Chevron bracing location matrix and **n** is the measurement noise. The numerical values of the parameters of the nonlinear time-varying dynamical system are discussed in the following section.

Parameter setting

Damage scenario. A total of 11 damage scenarios are considered in this article. First, two input signals are applied to the structure employing an MR damper. The first input signal is a random earthquake signal and the second input is a random current signal (converted

Table 1. Damage scenarios.

Damage case	Damage location	Damage severity (%)
0	N/A	N/A
1	First floor	5
2	First floor	10
3	First floor	15
4	First floor	30
5	First floor	50
6	Second floor	5
7	Second floor	10
8	Second floor	15
9	Second floor	30
10	Second floor	50

Table 2. Parameters for SD-1000 MR damper model.

Parameter	Value	Parameter	Value
c_{0a}	21.0 N s/cm	α_a	140 N/cm
c_{0b}	3.50 N s/cm V	α_b	695 N/cm V
k_0	46.9 N/cm	γ	363 cm^{-2}
c_{1a}	283 N s/cm	β	363 cm^{-2}
c_{1b}	2.95 N s/cm V	A	301
k_1	5.00 N/cm	N	2
x_0	14.3 cm	η	190 s^{-1}

MR: magnetorheological.

from the voltage). The measured quantities are velocity responses of the first- and second-floor levels in the smart building. Damage is simulated by the stiffness decrease at the first- and second-floor levels. Although a variety of damage scenarios need to be considered, for example, stiffness, structural damping coefficients, sensor faults (Sharifi et al., 2010), and damper faults (Yun and Masri, 2008, 2009), we only considered the stiffness degradation. Other factors will be taken into account in our future studies. For each set of input signals, 11 damage scenarios are considered as shown in Table 1. Damage case 0 corresponds to no damage. The 5% damage located at the first floor, for example, implies that the stiffness at the first floor of the smart structure is decreased by 5%. All other damage cases are similarly defined.

For each damage case, 100 simulations were performed to generate a total of 100 sets of structural responses. Consequently, a total of 1100 numerical simulations are conducted (11 cases by 100 tests = 1100 simulations). For each data set, 50 data sets are used for training the DSFs, while the other 50 data sets are used for validating the trained models. Second, the DWT is applied to the numerical data sets. The DWT reduces the computational loads and filters noise from the measured data. Then, the wavelet-filtered responses are estimated using AR time series models. Once the WAR is constructed, the AR coefficients from the WAR model are extracted to identify structural damage. Finally, the extracted features are inputted to the proposed multiclass SVM algorithm.

Simulation parameters. The second-level wavelet signals are used for estimating the AR models. The method uses Daubechie wavelets for low-frequency decomposition in order to denoise and compress the response data. The initial AR model order was selected to 100 after many trial and error simulations. The properties of a three-story building structure are given as follows: the mass of each floor $m_1 = m_2 = m_3 = 98.3$ kg; the stiffness of each story $k_1 = 516{,}000$ N/m, $k_2 = 684{,}000$ N/m, and $k_3 = 684{,}000$ N/m; and damping coefficients of each floor $c_1 = 125$ N s/m, $c_2 = 50$ N s/m, and $c_3 = 50$ N s/m. The properties of the SD-1000 MR damper are given in Table 2. Based on this building–MR damper system, a set of dynamic responses is collected for use in developing the WAR model.

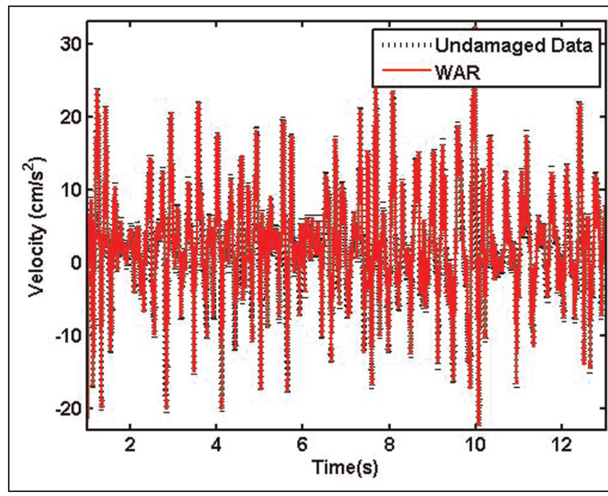

Figure 6. Comparison of the WAR model and undamaged smart structures.
WAR: wavelet-based autoregressive.

Classification results

Wavelet-compressed AR modeling. To construct the wavelet-filtered AR models (WAR), displacements, velocities, and acceleration responses are measured. Figure 6 compares a sample WAR model with the measured velocity data obtained from the undamaged structure. Figure 7 depicts the result of the WAR modeling using the time history responses obtained from the damaged smart structure.

It is shown from these figures that the proposed WAR model effectively predicts the original data. To quantify the estimation performance, a variety of evaluation indices are used. The first evaluation index is the maximum error

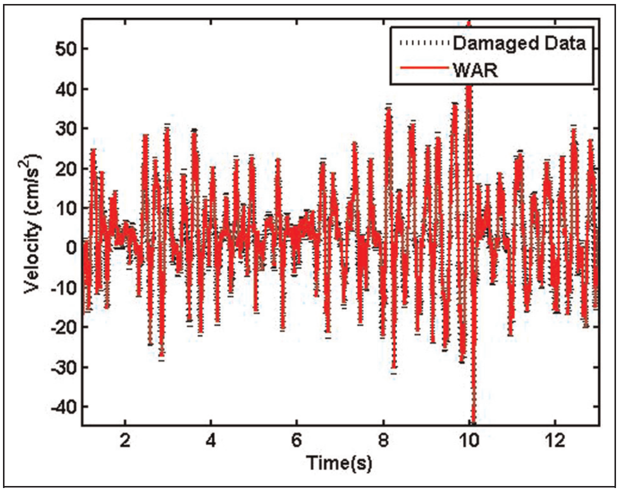

Figure 7. Comparison of the WAR model and damaged smart structures.
WAR: wavelet-based autoregressive.

$$J_1 = \max|\hat{y} - \tilde{y}| \quad (34)$$

where $\hat{y}$ is the estimation and $\tilde{y}$ is the actual structural response data. The second evaluation index is

$$J_2 = \min|\hat{y} - \tilde{y}| \quad (35)$$

As the third evaluation index, the root mean square error (RMSE) is used

$$J_3 = \text{RMSE} = \sqrt{\frac{\sum|\hat{y} - \tilde{y}|^2}{N}} \quad (36)$$

where N is the number of data points. As the fourth evaluation index, the fitting rate (FR) is adopted as

$$J_4 = FR = \left[1 - \frac{\text{var}(\tilde{y} - \hat{y})}{\text{var}(\tilde{y})}\right] \times 100 \quad (37)$$

where "var" represents variance of data. If a perfect agreement exists between the trained model and the original data, FR will be 100. The last evaluation index is the computational load given by

$$J_5 = \text{CPU time} \quad (38)$$

Table 3 provides the training results, including the error between the trained model and the actual response of the smart structure using the AR model and WAR model.

It is clearly observed from this table that the computational load of AR modeling is significantly reduced by adopting the wavelet-filtering process without scarifying modeling accuracy, that is, the computation load of the AR modeling is four times higher than the WAR model's training time. Thus, the WAR model is used in developing the proposed SHM scheme for the smart structures in this article. As previously discussed, there are a variety of effective DSFs in the field of SHM, for example, eigenvalues, eigenvectors, and influence lines, to name a few. However, they are not appropriate for damage detection of nonlinear dynamical systems. The reason is that such approaches have been applied based on the assumption that the structure under investigation is LTI. One of the most effective methods in detecting damage in nonlinear dynamical systems is the RFM (Yun and Masri, 2008, 2009). As a nonparametric identification technique, the RFM coefficients (in particular, orthogonal coefficients) can be used as an effective change indicator in an MR damper. Although the effectiveness of the RFM approach is promising, it requires forces to be measured from MR dampers using load cells. Certainly, it will be challenging to use the RFM when the force measurement is not readily available. Thus, central goal of this article is to detect dynamic changes in nonlinear systems using only structural response measurements. The proposed method can be applied to nonlinear dynamical systems without information about the input force signals by employing only the AR time series models. The proposed approach is also robust against measurement noise due to utilization of the wavelet transform. At present, it is difficult to interpret the physical meaning of the detected changes. Such an issue could be addressed by integrating the proposed method with the RFM (Yun and Masri, 2008, 2009).

Multiclassification. The multiclass SVM classifier with one-versus-the-rest classification method (see section "Multiclass classification") is used in this article. On a

Table 3. Training results and their associated errors.

	J_1	J_2	J_3	J_4	J_5
WAR					
Undamaged system	2.8760	1.154e−4	1.2522	99.1574	1.5858
Damaged system	4.3929	3.054e−4	3.1955	99.2441	1.6079
AR					
Undamaged system	1.9586	0.0011	0.3693	99.6738	6.8998
Damaged system	3.1250	8.796e−4	0.9218	99.7170	7.0238

WAR: wavelet-based autoregressive; AR: autoregressive.

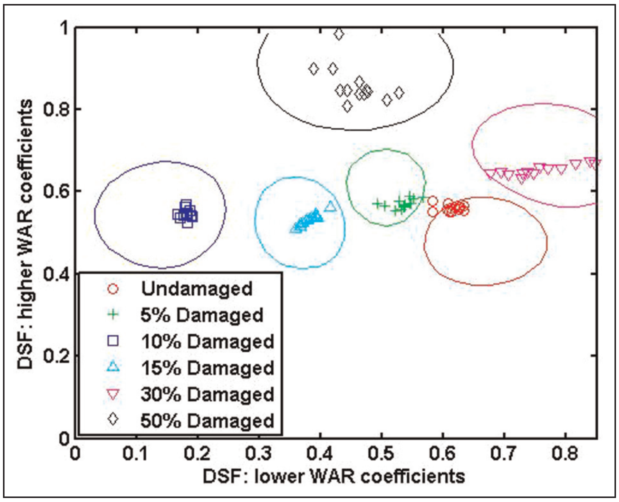

Figure 8. Trained multiclassification: case 0–case 5.
DSF: damage-sensitive feature; WAR: wavelet-based autoregressive.

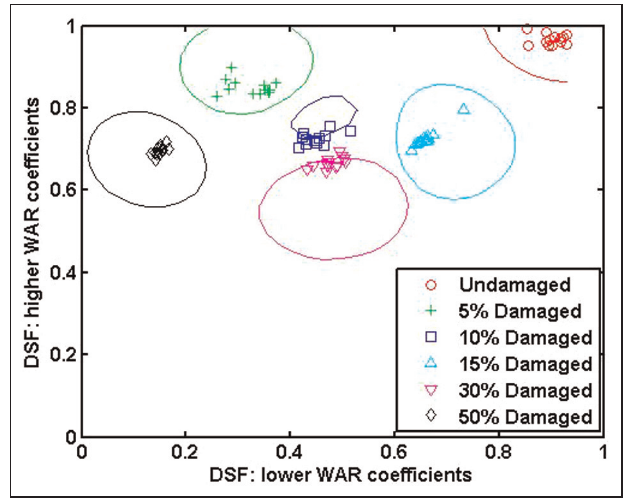

Figure 9. Trained multiclassification: case 6–case 10.
DSF: damage-sensitive feature; WAR: wavelet-based autoregressive.

two-dimensional plot, drawing of DSF values of large and small WAR coefficients in some cases produces a circle or elliptical shape (see Figure 8). In pattern recognition, the Gaussian or polynomial kernel is known to be well suited for capturing circle or elliptical shapes (Nguyen et al., 2005). Furthermore, the Gaussian kernel SVM has an attractive feature of effective learning capability (Wang et al., 2003). Hence, Gaussian kernels with the parameter set $(C_{\mathrm{SVM}}, \sigma)$ are applied. First, the multiclass SVM classifier is trained using the training data to derive the decision boundaries that classify the training data set with a concept of margin. The *margin* is defined as the smallest distance between any of the training data and the decision boundary in section "Multiclass classification." Hence, each decision boundary is formed by solving equations (4) and (5) in a way such that it divides one class from the other classes with the maximum margin. The parameter set $(C_{\mathrm{SVM}}, \sigma)$ of the Gaussian kernel affects the formation of the decision boundaries. The classification performance is also affected by $(C_{\mathrm{SVM}}, \sigma)$. Hence, the optimal parameter sets $(C^*_{\mathrm{SVM}}, \sigma^*)$ need to be found that minimize misclassification errors, where the *misclassification error* is defined as the difference between the classified classes and the target classes. Cross-validation and the grid search algorithm are adopted to find $(C^*_{\mathrm{SVM}}, \sigma^*)$ (Hsu et al., 2010). The DSF values are normalized by dividing them by the maximum DSF values in lower and higher WAR coefficients. Using fivefold cross-validation within the grid pairs of $(C_{\mathrm{SVM}} = 2^{-5}, \ldots, 2^{15}$ and $\sigma = 2^{-15}, \ldots, 2^{15})$, $C^*_{\mathrm{SVM}} = 1$ and $\sigma^* = 25$ are obtained.

Figure 8 shows the simulation results on the multiclassification training of the nonlinear time-varying structural system with various damage scenarios at the first-floor level using the SVM (case 0–case 5). As shown in Figure 8, almost all the samples remain

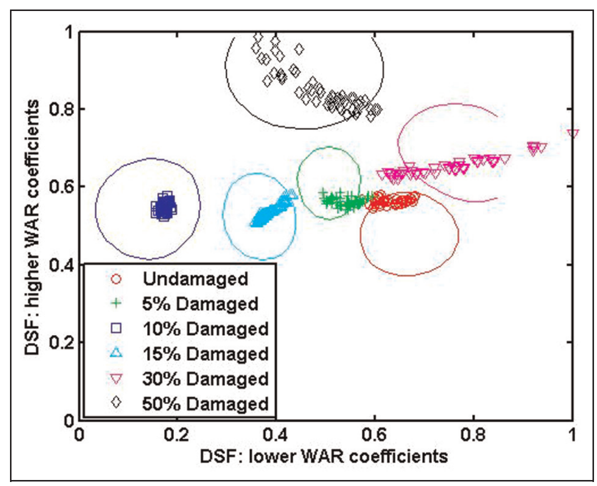

Figure 10. Validation: case 0–case 5.
DSF: damage-sensitive feature; AR: autoregressive.

within the SVM boundaries, except for the undamaged case. Figure 9 depicts the classification results of various damage statuses at the second-floor level. It is noted that the second-floor damage features are better distinguished than the first-floor damage features from the healthy case. The reason is that the MR damper is installed on the first-floor level, and thus, the change in the physical properties of the first floor (i.e. stiffness and damping) is affected by the operation of the MR damper as well as the structural damage. Boundaries can be made tighter by increasing the value of $(C_{\mathrm{SVM}}, \sigma)$, although doing so leads to more complex boundaries, which results in degraded validation performance. In this study, the trained models are updated, based on the validation results.

The simulation results with validation data sets are depicted in Figures 10 and 11. As shown in these figures, the trained SVM models effectively classify most

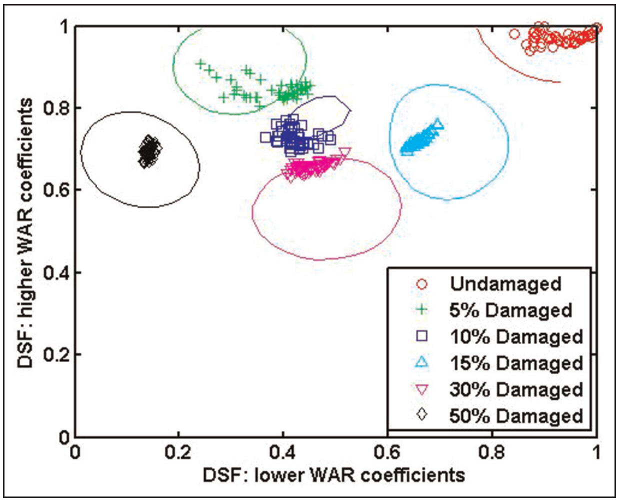

Figure 11. Validation: case 6–10.

damage cases, except for some samples of the undamaged and 5% first-floor damage cases. In Figure 10, it is observed that the distinction in the healthy and 5% damaged classes is ambiguous because the DSF values are normalized by the maximum DSF value (i.e. Max_DSF). For example, the difference of 0.1 between the healthy and 5% damaged DSF values represents the difference between two normalized DSF values. Hence, the actual difference that is corresponding to the 0.1 value is equal to 0.1 × Max_DSF, which is not a small difference. To clearly visualize the distinction, the 5% damage part is magnified. As shown in Figure 10, all the data points obtained from the healthy system belong/close to the healthy decision boundary, except a single data sample. Two data samples among the 5% damage data set do not belong/close to the 5% damage decision boundary. It is noted that the classification is determined by comparison of the distance between a specific data point and decision boundaries: the data samples out of six boundaries are assigned to one of the classes having the maximum value in equation (10). For example, if the distance between a data point and the healthy decision boundary is shorter than the one between the data point and the 5% decision boundary, the data sample is assigned to the healthy class. The SVM model was trained with 78 data samples (6 classes × 13 samples/class) as shown in Figure 8 and then tested with 248 data samples (6 classes × 48 samples/class) as shown in Figure 10. Three data samples (one undamaged and two 5% damaged data) among the 248 data samples are misclassified, which means the SVM shows the classification performance with the accuracy of 98.96%. As the data samples for training the SVM increase, the classification accuracy increases as shown in Table 4. When the SVM is trained with 120 data samples instead of 78 samples, only two data samples are misclassified while the computational complexity also increases.

Table 4. Validation errors.

Number of training data	Number of errors	
	Naive Bayes	NMSVM
36 (= 6 data/class × 6 classes)	10	4
78 (= 12 data/class × 6 classes)	5	3
120 (= 20 data/class × 6 classes)	4	2

NMSVM: nonlinear multiclass support vector machine.

However, as a matter of fact, it is very challenging to detect the 5% change in the stiffness from smart buildings because the stiffness and damping values change over time due to the operation of the smart control devices. Furthermore, in practice, the 5% difference in the stiffness is too small to identify some damages using vibration data. The statistical analysis obtained from the field testing and extensive simulations shows that the normal environmental change (e.g. temperature fluctuation) accounts for variations in frequencies with variance from 0.20% to 5%. These noise effects may mask the frequency changes caused by structural damage (Doebling and Farrar, 1997; Ko and Ni, 2005; Ni et al., 2005; Sohn et al., 1998; Sohn et al., 2000). Hence, it is recommended by field engineers that the stiffness reduction below 10% is considered too low to be distinguished (Bulut et al., 2005). In the authors' opinion, such issues could be partially addressed by the following: (1) Changing the multiclassification into binary classification—for instance, the healthy features and the 5% damage features can be assigned as 0 and 1, respectively. (2) Increasing the number of data samples—increasing sample size would boost the statistical power of the decision-making, for example, as the feature samples increase, the misclassification errors will decrease. (3) Utilizing different normalization schemes—in general, normalization schemes play an important role in feature extractions for SHM (Sohn and Farrar, 2000). (4) Selecting different combinations of the lower and higher WAR coefficients—for instance, the first 5 WAR coefficients can be used for selecting the lower WAR coefficients, instead of the first 10 coefficients. Such a different selection would lead to reduction in the ambiguous distinctions between the 5% damage and healthy classes, although the performance of other classes could degrade. In other words, the performance of a specific classification (e.g. 5% damage) can be significantly improved by sacrificing other classes. (5) Applying data fusion scheme—for instance, by adding a Z-axis (torsional modes) into the X–Y axis (lower and higher WAR coefficients obtained from the translational modes), a better decision-making model could be constructed. As another example, the lower DSF values (damage features) can be divided into two groups, then the SVM can use three damage features, including lower DSFs, medium DSFs, and higher DSFs. Such additional feature would enhance the performance of the SVM-based classification algorithm while also increase the cost of higher computational complexity. Thus, the authors of this article considered to use only two features in order to reduce the computational complexity while maintain the classification performance. (6) Adopting different measurements—for instance, the use of the Lamb waves instead of vibration signals would reduce the environmental conditions (Park et al., 2006; 2007).

In addition, to demonstrate the effectiveness of the proposed SVM approach, the validation errors are compared with the results from the NB as shown in Table 4. As shown in this table, the proposed approach has fewer errors than the NB method. In particular, it is shown that the performance of the proposed SVM is more robust than that of the NB approach when many data points are not available.

Conclusion

This article proposes the use of a NMSVM for SHM of nonlinear time-varying structures. The SHM framework is developed through the integration of the NMSVM, DWT, AR models, and DSFs: (1) Dynamic responses of a structure equipped with a highly nonlinear hysteretic smart control device are identified using the WAR time series models. (2) DSFs are extracted from the WAR models derived from both damaged and undamaged smart structures. The DSF is expressed in terms of the AR coefficients, which are related to the frequencies (or eigenvalues) of smart structures. (3) The damage is detected by observing the migration of the extracted AR coefficients and NMSVM. To demonstrate the effectiveness of the proposed WAR-NMSVM approach, a three-story building equipped with an MR damper is investigated. In addition, the performance of the proposed NMSVM is compared with that of the NB classification technique as a baseline. It is demonstrated from the simulation that the proposed SHM framework is effective in identifying the damage of smart structural systems equipped with time-varying nonlinear MR dampers.

Declaration of conflicting interests

The authors declared no potential conflicts of interest with respect to the research, authorship, and/or publication of this article.

Funding

This research received no specific grant from any funding agency in the public, commercial, or not-for-profit sectors.

References

Adeli H and Saleh A (1999) *Control, Optimization, and Smart Structures: High-Performance Bridges and Buildings of the Future*. New York: John Wiley & Sons, Inc.

Ankireddi S and Yang HTY (1999) Neural networks for sensor fault correction in structural control. *ASCE Journal of Structural Engineering* 125: 1056–1064.

Arsava SK, Kim Y, El-Korchi T and Park HS (2013a) Identification of high impact responses in smart structures. *Journal of Smart Materials and Structures* 22(5): 1–30.

Bulut A, Singh AK, Shin P, et al. (2005) Real-time nondestructive structural health monitoring using support vector machines and wavelets. *Proceedings of SPIE* 5770: 180–189.

Burges CJC (1998) A tutorial on support vector machines for pattern recognition. *Data Mining and Knowledge Discovery* 2: 121–167.

Carden PE and Brownjohn JMW (2007) ARMA modelled time series classification for structural health monitoring. *Mechanical Systems and Signal Processing* 22: 295–314.

Chen PH, Shen HK, Lei CY, et al. (2012) Support vector machine-based method for automated steel bridge rust assessment. *Automation in Construction* 23: 9–19.

Dyke SJ, Spencer BF Jr, Sain MK, et al. (1996) Modeling and control of magnetorheological dampers for seismic response reduction. *Smart Materials and Structures* 5: 565–575.

Hayano H and Mita A (2005) Structural health monitoring system using FBG sensor for simultaneous detection of acceleration and strain. *Proceedings of SPIE* 5765: 624–633.

He HX and Yan WM (2007) Structural damage detection with wavelet support vector machine: introduction and applications. *Structural Control and Health Monitoring* 14: 162–176.

Hsu C-W, Chang C-C and Lin C-J (2010) *A Practical Guide to Support Vector Classification* (technical report). Taipei, Taiwan: Department of Computer Science, National Taiwan University.

Hurlebaus S and Gaul L (2006) Smart structure dynamics. *Mechanical Systems and Signal Processing* 20: 255–281.

Kim Y, Hurlebaus S, Sharifi R, et al. (2009a) Nonlinear identification of MIMO smart structures. In: *ASME dynamic systems and control conference*, Hollywood, CA, 12–14 October.

Kim Y, Langari R and Hurlebaus S (2009b) Semiactive nonlinear control of a building structure equipped with a magnetorheological damper system. *Mechanical Systems and Signal Processing* 23: 300–315.

Kim Y, Langari R and Hurlebaus S (2011) MIMO fuzzy identification of building-MR damper systems. *International Journal of Intelligent and Fuzzy Systems* 22: 185–205.

Kim Y, Kim C and Langari (2010a) Novel bio-inspired smart control for hazard mitigation of civil structures. *Journal of Smart Materials and Structures* 19(11): 1–12.

Kim Y, Langari R and Hurlebaus S (2010b) Model-based multi-input, multi-output supervisory semiactive nonlinear fuzzy controller. *Computer-Aided and Infrastructure Engineering* 25: 387–393.

Kim Y, Hurlebaus S, and Langari R (2010c) Control of a seismically excited benchmark building using linear matrix inequality-based semiactive nonlinear fuzzy control ASCE. *Journal of Structural Engineering* 136: 1023–1026.

Kim Y, Chong JW, Con K and Kim JM (2013b) Wavelet-based AR-SVM for health monitoring of smart structures. *Journal of Smart Materials and Structures* 22(1): 1–12.

Ko JM and Ni YQ (2005) Technology developments in structural health monitoring of large-scale bridges. *Engineering Structures* 27: 1715–1725.

Li Z, Koh BH and Nagarajaiah S (2007) Detecting sensor failure via decoupled error function and inverse input-output model. *ASCE Journal of Engineering Mechanics* 133: 1222–1228.

Lu KC, Loh CH, Yang YS, et al. (2008) Real-time structural damage detection using wireless sensing and monitoring system. *Smart Structures and Systems* 4: 759–778.

Mainmon O and Rokach L (2010) *Data Mining and Knowledge Discovery Handbook*. New York: Springer.

Mita A and Hagiwara H (2003) Quantitative damage diagnosis of shear structures using support vector machine. *KSCE Journal of Civil Engineering* 7: 683–689.

Mita A and Taniguchi R (2004) Active damage detection method using support vector machine and amplitude modulation. *Proceedings of SPIE* 5391: 21–29.

Mitchell R, Kim Y, and El-Korchi T (2012) System identification of smart structures using a wavelet neuro-fuzzy model. *Journal of Smart Materials and Structures* 21(11): 1–12.

Mitchell R, Kim Y, El-Korchi T, et al (2012) Wavelet-neuro-fuzzy control of hybrid building-active tuned mass damper system under seismic excitations. *Journal of Vibration and Control* 19(12): 1881–1894.

Nagarajaiah S and Spencer BF Jr (2003) State of the art of structural control. *ASCE Journal of Structural Engineering* 129: 845–856.

Nair KK and Kiremidjian AS (2007) Time series based structural damage detection algorithm using Gaussian mixtures modeling. *Transactions of the ASME: Journal of Dynamic Systems Measurement and Control* 129: 285–293.

Nair KK, Kiremidjian AS and Law KH (2006) Time series-based damage detection and localization algorithm with application to the ASCE benchmark structure. *Journal of Sound and Vibration* 291: 349–368.

Nguyen X, Jordan MI and Sinopoli B (2005) A kernel-based learning approach to ad hoc sensor network localization. *ACM Transaction on Sensor Networks* 1: 134–152.

Ni YQ, Hua XG, Fan KQ, et al. (2005) Correlating modal properties with temperature using long-term monitoring data and support vector machine technique. *Engineering Structures* 27: 1762–1773.

Oh CK and Sohn H (2009) Damage diagnosis under environmental and operational variations using unsupervised support vector machine. *Journal of Sound and Vibration* 325: 224–239.

Park S, Lee JJ, Yun CB, et al. (2007) A built-in active sensing system-based structural health monitoring technique using statistical pattern recognition. *Journal of Mechanical Science and Technology* 21: 896–902.

Park S, Yun CB, Roh Y, et al. (2006) PZT-based active damage detection techniques for steel bridge components. *Journal of Smart Materials and Structures* 15: 957–966.

Sharifi R, Kim Y and Langari R (2010) Sensor fault isolation and detection of smart structures. *Smart Materials and Structures* 19: 105001.

Shimada M and Mita A (2005) Damage assessment of bending structures using support vector machine. *Proceedings of SPIE* 5765(923): 923–930.

Shimada M, Mita A and Feng MQ (2006) Damage detection of structures using support vector machines under various boundary conditions. *Proceedings of SPIE* 6174: 6174K1–6174K9.

Sohn H and Farrar CR (2000) Statistical process control and projection techniques for structural health monitoring. In: *European COST F3 conference on system identification & structural health monitoring*, Madrid, 6–9 June.

Sohn H, Czarnecki JA and Farrar CR (2000) Structural health monitoring using statistical process control. *ASCE Journal of Structural Engineering* 126: 1356–1363.

Sohn H, Dzwonczyk M, Straser EG, et al. (1998) Adaptive modeling of environmental effects in modal parameters for damage detection in civil structures. In: *Smart systems for bridges, structures, and highways (proceedings of SPIE)*, vol. 3325, San Diego, CA, 4–5 March, pp. 127–138. Bellingham, WA: SPIE.

Spencer BF Jr, Dyke SJ, Sain MK, et al. (1997) Phenomenological model for magnetorheological dampers. *ASCE Journal of Engineering Mechanics* 123: 230–238.

Vines-Cavanaugh D, Cao Y and Wang ML (2010) Support vector machine for abnormality detection on a cable-stayed bridge. *Proceedings of SPIE* 7647: 76471T1–76471T11.

Wang W, Xu Z, Lu W, et al. (2003) Determination of the spread parameter in the Gaussian kernel for classification and regression. *Neurocomputing* 55: 643–663.

Yun HB and Masri SF (2008) Stochastic change detection in uncertain nonlinear systems using reduced-order models: system identification. *Journal of Smart Materials and Structures* 17: 015040.

Yun HB and Masri SF (2009) Stochastic change detection in uncertain nonlinear systems using reduced-order models: classification. *Journal of Smart Materials and Structures* 18: 015004.